

Mean-field calculations of charge radii in ground and isomeric states of Cd isotopes

P. Sarriguren*

Instituto de Estructura de la Materia, IEM-CSIC, Serrano 123, E-28006 Madrid, Spain

(Dated: November 12, 2019)

Quadrupole moments and charge radii in cadmium isotopes are studied from a microscopic perspective. The results obtained from self-consistent deformed Hartree-Fock+BCS calculations with Skyrme forces are compared with isomer and isotope shifts measured from high resolution laser spectroscopy experiments. The microscopic calculations reproduce fairly well the main features observed in those isotopes that include the linear increase with the neutron number of the quadrupole moments of the $11/2^-$ isomers, as well as the parabolic behavior of the mean-square charge radii difference between isomers and ground states.

I. INTRODUCTION

The theoretical and experimental study of the isotopic evolution of ground and low-lying state properties in nuclei has revealed over the years to be a very sensitive tool to study highly topical issues in nuclear structure physics, such as shell evolution, shape coexistence phenomena or shape transitions [1–4]. In particular, charge radii and electromagnetic moments are very suitable quantities to learn about the nuclear structure properties. A great experimental effort has been devoted to determine the nuclear charge radii. A review of the state of knowledge can be found in Ref. [5], where different types of experimental data have been compiled. These include absolute radii measured by muonic-atom spectra and electron scattering experiments, as well as relative radii determined from isotope shifts. The same is true for the nuclear electromagnetic moments that can be found, for example, in the tabulation of Ref. [6] and references therein.

Cadmium isotopes in the neutron mid-shell region have received increasing attention as examples where intruder excitations appear. In fact, the entire region around $Z=50$ has been subject of discussions [7–9] concerning the origin of the low-lying excitations. At first, even-even Cd isotopes were considered clear examples of vibrational nuclei, but this picture was later questioned by the presence of intruder states opening the possibility of shape coexistence phenomena. Models that include mixing between intruders and phonon states were used to explain the spectroscopic properties of these isotopes. Detailed spectroscopic investigations carried out more recently (see Ref. [7] for a review) questioned the robustness of the spherical vibrator picture for these nuclei, suggesting to be deformed γ -soft rotors. The issue of the nature of these excitations remains an open problem.

Recently, high precision electromagnetic moments and charge radii have been measured in Cd isotopes ($Z = 48$) with the collinear laser spectroscopy setup at the ISOLDE-CERN radioactive ion beam facility [10–13]. This is a region of special interest because of its proximity

to the shell closure at $Z = 50$. In Ref. [10], quadrupole moments in neutron-rich $A = 107 - 129$ Cd isotopes were studied. The hyperfine structure was used to identify a spin $1/2^+$ ground-state in $^{111-119}\text{Cd}$ isotopes and $3/2^+$ in $^{121-129}\text{Cd}$. Long-lived isomeric states with spin-parity assignments $11/2^-$ were also firmly established in all of these isotopes. The study was extended to lighter odd- A Cd isotopes ($A = 101 - 109$) in Ref. [12], where ground-state spins $5/2^+$ were assigned to them and electromagnetic moments were measured. The most remarkable finding in those works was a linear increase of the quadrupole moments of the isomeric $11/2^-$ states with the number of neutrons. A plain explanation of this feature was offered within the extreme shell model, but the increase was experimentally found well beyond the single $h_{11/2}$ shell. The simplicity of the linear increase was investigated microscopically within the covariant density functional theory [14] and it was found to be related to the pairing correlations, which smear out the changes induced by the single-particle shell structure, leading to a smooth shape evolution.

In two subsequent papers [11, 13] the charge radii of Cd isotopes were also studied by high-resolution laser spectroscopy measurements. In Ref. [13], isotope shifts were used to determine the differences in mean-square nuclear charge radii of $^{100-130}\text{Cd}$ isotopes. The extracted root-mean-square charge radii show a smooth parabolic behavior on top of a linear trend and a regular odd-even staggering. The main features of these measurements were not reproduced in detail by standard density functional theory, but were well accounted for by a new Fayans functional, which includes a gradient term in the pairing functional [15] as a distinctive aspect.

In Ref. [11] isomer shifts were determined in $^{111-129}\text{Cd}$ odd- A isotopes. Mean-square charge radii differences between the $11/2^-$ isomer states and the ground states ($1/2^+$ or $3/2^+$) were measured. They were shown to exhibit a parabolic behavior as a function of the neutron number. This feature was interpreted in terms of a simple model that takes into account the existing link between the nuclear radii and the quadrupole deformation of the various states. The parabolic behavior arises naturally from the previously established [10] linear increase of the deformation parameter in the isomeric $11/2^-$ states together with the practically constant and small deforma-

*Electronic address: p.sarriguren@csic.es

tion of the ground states. The results of this simple model were supported by relativistic mean-field calculations.

The purpose of this paper is to study the charge radii, the quadrupole moments, and their correlations to see whether those simple properties observed experimentally and mentioned above, emerge naturally from microscopic calculations based on a nonrelativistic self-consistent mean-field formalism with Skyrme effective nucleon-nucleon interactions and pairing correlations in the BCS approximation. Beyond mean-field calculations have already been carried out to study the evolution of the low-lying excitation energies and transition strengths in Cd isotopes [16]. The formalism used there involves a mean-field calculation with the finite range Gogny interaction, including particle number and angular momentum projections, as well as configuration mixing in the generator coordinate method. A different approach has also been explored in Ref. [17], where an IBM Hamiltonian was constructed to study the spectroscopy of Cd isotopes, based on a mapping of the triaxial energy surfaces obtained from constrained Skyrme self-consistent mean-field calculations. Similar calculations [18, 19] in other mass regions have shown the possibilities of that method. A full understanding of the spectroscopic properties of Cd isotopes will require in one way or another going beyond the mean-field approach. However, the question to answer in this paper is to what extent a simple approach based on a self-consistent mean field with standard Skyrme forces can reproduce the main features observed experimentally on charge radii and quadrupole moments of ground and isomeric states in Cd isotopes.

The paper is organized as follows: In the next section, the ingredients of the theoretical formalism used to calculate the nuclear properties are presented. Section III and IV contain the results obtained for quadrupole moments and charge radii, respectively. Section V contains the conclusions of the work.

II. THEORETICAL APPROACH

The theoretical formalism used in this work is based on a self-consistent deformed Hartree-Fock (HF) mean-field calculation with effective two-body density-dependent Skyrme interactions, including pairing correlations in the BCS approximation. Single-particle energies, wave functions, and occupation probabilities are generated from this mean field. The virtues of this type of self-consistent microscopic formalisms are well known. They include the universality of the Skyrme density functional that allows one to use the same interaction throughout the entire nuclear chart. The reliability of such interactions also implies a great predictive power to those calculations.

The Skyrme interaction SLy4 [20] is used in this work as a representative reference of the Skyrme forces. For comparison, I also consider the parametrization SkM* [21], which is also a reliable standard reference for Skyrme forces. Actually, one can find in the literature hundreds

of Skyrme interactions, see for example Ref. [22], where 240 different parametrizations available at that time were considered. No doubt, other more sophisticated Skyrme interactions could be used for the present study than those used here, but most of these new constructed interactions have been especially designed and adjusted to treat specific nuclear properties. Therefore, in this work I preferred to check the properties of Cd isotopes with standard and classical Skyrme forces with a proven wide range of applicability that have been successfully tested throughout the nuclear chart for a large variety of different nuclear properties [23]. This is the case of the forces considered SkM* and SLy4. SkM* is based on an accurate description of nuclear ground states properties like radii and multipole moments, as well as surface energies and fission barriers. On the other hand, SLy4 was developed to describe properly neutron-rich nuclei. These two forces are still meaningful references with which new developed Skyrme interactions are compared.

The solution of the HF equation, assuming time reversal and axial symmetry, is found by using the formalism developed in Ref. [24]. The single-particle wave functions are expanded in terms of the eigenstates of an axially symmetric harmonic oscillator in cylindrical coordinates, using twelve major shells. The two parameters of the cylindrical basis related to the oscillator length and the ratio of the axes are chosen optimally to minimize the energy. It is also worth noting that, contrary to the shell model approach where a restricted valence space is used, in this approach a large basis space is used and therefore, core polarization effects are fully taken into account without effective charges.

The method also includes pairing between like nucleons in the BCS approximation with fixed gap parameters for protons and neutrons [24], which are determined phenomenologically from the odd-even mass differences through a symmetric five-term formula involving the experimental binding energies when available [25]. In those cases where experimental information for masses is still not available, the same pairing gaps as the closer isotopes measured are used. Given the importance that pairing correlations have in the microscopic explanation of both quadrupole moments [14] and charge radii [13] in the Cd isotopes, I also show for comparison in some instances, the results obtained with a fixed pairing strength $G_{p,n}$, parametrized with a standard dependence on Z and N . The BCS equations are solved at the end of each HF iteration, generating occupation probabilities of the single-particle states that are included in the next HF iteration. Thus, the HF+BCS problem is solved self-consistently.

In a further step, constrained HF calculations are performed with a quadratic constraint [26], minimizing the energy under the restriction of keeping the nuclear deformation fixed. The resulting plots of the total energy versus deformation give the landscapes of nuclear stability and are called deformation-energy curves (DECs).

Figure 1 shows the DEC's for even-even $^{98-130}\text{Cd}$ isotopes that are obtained from constrained HF+BCS cal-

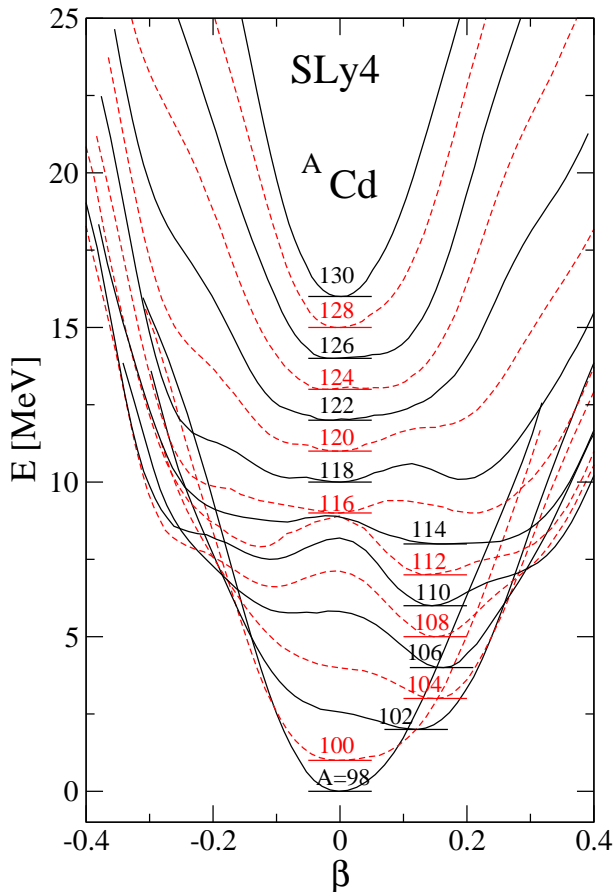


FIG. 1: Deformation-energy curves for even-even $^{98-130}\text{Cd}$ isotopes obtained from constrained HF+BCS calculations with the Skyrme force SLy4.

culations with the Skyrme force SLy4 and pairing correlations treated in the fixed-gap approach. The results are shown as a function of the quadrupole deformation parameter β calculated as $\beta = \sqrt{\pi/5}Q_0/(A\langle r^2 \rangle)$, which is defined in terms of the intrinsic quadrupole moment Q_0 and the nuclear mean-square radius $\langle r^2 \rangle$ defined later. The DEC's have been scaled to the energy of their ground states and have been shifted by 1 MeV from one isotope to the next one, starting from the lightest one.

The isotopes studied start and end at neutron magic numbers, $A = 98$ ($N = 50$) and $A = 130$ ($N = 82$), respectively. It is observed that the spherical shapes at shell closures evolve to deformed shapes in the isotopes between them. First, as the number of neutrons increases, a prolate shape is developed with quadrupole deformations between $\beta = 0.1$ and $\beta = 0.2$. Around middle shell, between $A = 116$ and $A = 126$, the DEC's are rather shallow with deformations in the range of $-0.2 < \beta < 0.2$ that result practically degenerate in energy. Finally, spherical shapes are recovered as the shell closure at $A = 130$ is approached. Similar trends in the DEC's are obtained with other Skyrme forces, in particular, with the force SkM*. Thus, spherical, prolate,

and oblate configurations can be identified in the profiles of the energy curves of mid-shell Cd isotopes. However, these profiles are very soft with fairly shallow minima and shape coexistence could hardly be invoked. Rather they look like soft nuclei in this approach.

It is worth mentioning some existing works in this mass region based on mean-field approaches other than the present Skyrme HF + BCS calculations. In particular, mean-field studies of structural changes with the Gogny D1S interaction including triaxiality have been systematically carried out [27]. Triaxial landscapes have been also studied in Ref. [17] within Skyrme mean-field calculations and the interacting boson model. These calculations show that the axial prolate and oblate minima are quite soft in both axial and triaxial directions. Indeed, the oblate axial minima become saddle points when the γ degree of freedom is included in the analysis. The differences found in the axial equilibrium values between the present HF + BCS approach and those works are not significant.

In the case of odd- A nuclei, one-quasiparticle states are constructed by allowing the unpaired nucleon to occupy a single-particle state, which is blocked in the BCS calculation. The ground state is determined by finding the blocked state that minimizes the total energy. Quasiparticle excitations correspond to configurations with the odd nucleon in an excited state. In the present study the equal filling approximation is used, a prescription widely used in mean-field calculations to treat the dynamics of odd nuclei preserving time-reversal invariance [28]. In this approximation the unpaired nucleon is treated on an equal footing with its time-reversed state by sitting half a nucleon in a given orbital and the other half in the time-reversed partner. This approximation has been found [29] to be equivalent to the exact blocking when the time-odd fields of the energy density functional are neglected and therefore, it is sufficiently precise for most practical applications.

Because the spin and parity of the ground and low-lying excited states of the nuclei studied are known experimentally, the states to be blocked are chosen according to those assignments. In all cases the observed states have corresponding calculated states lying in the vicinity of the Fermi energy.

III. QUADRUPOLE MOMENTS

Figure 2 (a) shows the isotopic evolution in the even-even Cd isotopes of the quadrupole deformations β associated with the various minima shown in Fig. 1. Also shown in panel (b) are the quadrupole deformations of the odd- A isotopes. In this case the results for the ground states $5/2^+$ in $^{101-109}\text{Cd}$, $1/2^+$ in $^{111-119}\text{Cd}$, and $3/2^+$ in $^{121-129}\text{Cd}$, as well as the deformations of the $11/2^-$ isomer states in $^{111-129}\text{Cd}$ are shown. From this figure, the progress of deformations with the number of nucleons, which is already noticed in Fig. 1, is more apparent. De-

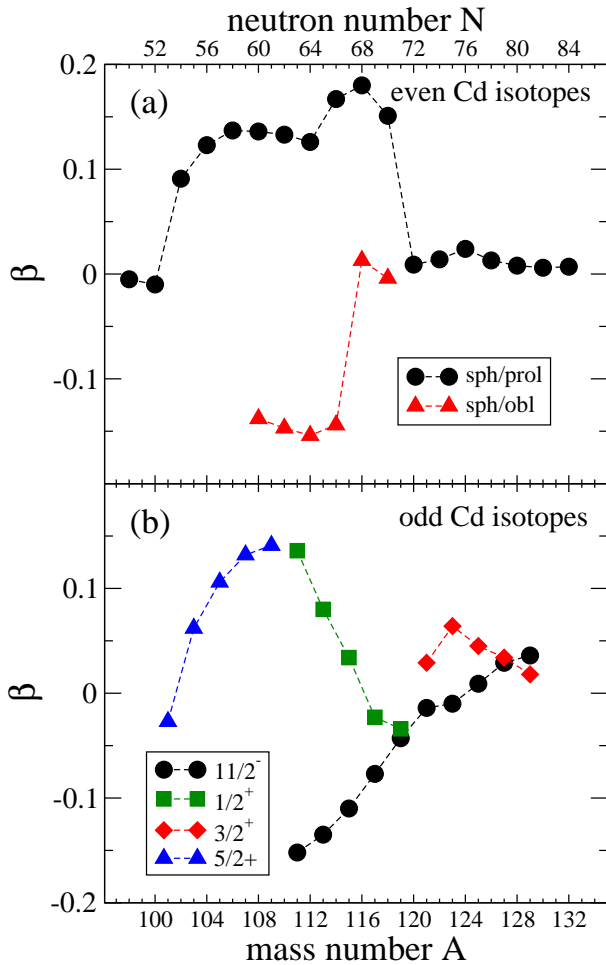


FIG. 2: Isotopic evolution of the quadrupole deformation β in even-even (a) and odd- A nuclei (b) evaluated with the SLy4 interaction.

formation increases as one departs from $N = 50$, developing prolate and oblate structures with $\beta \approx \pm 0.15$. These deformed configurations become again spherical when approaching the next shell closure at $N = 82$. These results agree with recent large-scale shell-model calculations in the light Cd isotopes [30].

In Fig. 3, instead of the quadrupole deformations β in the intrinsic system, the quadrupole moments in the laboratory frame are shown,

$$Q_{\text{lab}} = \frac{3K^2 - I(I+1)}{(I+1)(2I+3)} Q_0, \quad (1)$$

where Q_0 is the intrinsic quadrupole moment of the proton distribution,

$$Q_0 = \sqrt{\frac{16\pi}{5}} \int \rho_p(\vec{r}) r^2 Y_{20}(\Omega) d\vec{r}, \quad (2)$$

$\rho_p(\vec{r})$ is the density of protons in the nucleus, I is the total angular momentum and K stands for its projection

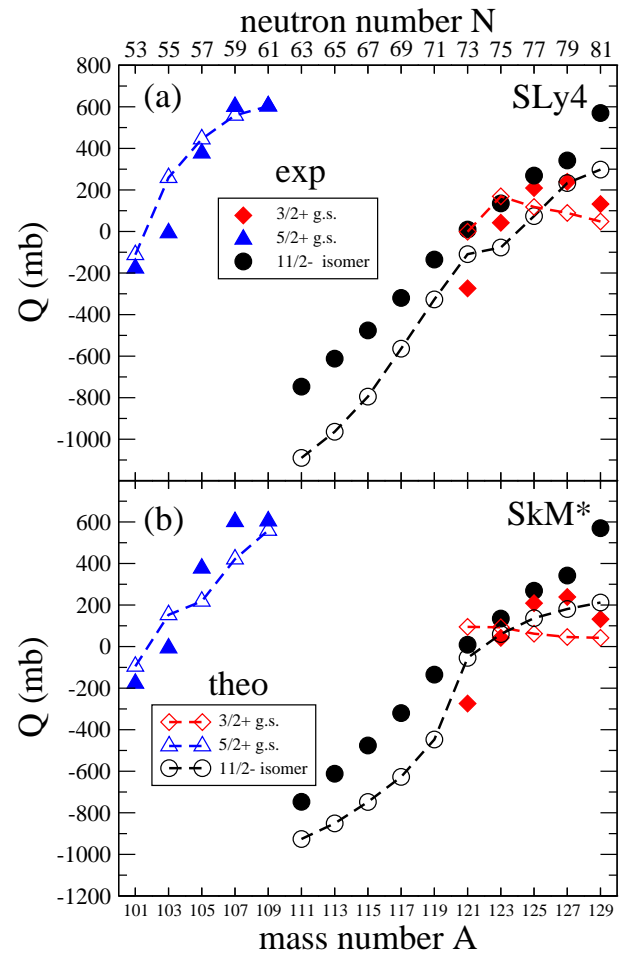


FIG. 3: Experimental quadrupole moments for the ground ($3/2^+$, $5/2^+$) and isomeric ($11/2^-$) states [10, 12], compared with HF+BCS calculations with SLy4 (a) and SkM* (b) interactions.

along the symmetry axis. The quadrupole moments are calculated within the HF+BCS approach with SLy4 (a) and SkM* (b) interactions. They are compared with the experimental values for the ground ($3/2^+$, $5/2^+$) and isomeric ($11/2^-$) states [10, 12]. Note that the quadrupole moments of the $1/2^+$ states vanish in the laboratory frame.

The isotopic linear increasing observed in the quadrupole moments of the $11/2^-$ isomeric states was interpreted in terms of a basic shell model in Ref. [10], splitting the total quadrupole moments into single-particle and core contributions. The data were reproduced with a simple fit $Q = ((120 - A)/9)Q_{\text{sp}} + Q_{\text{core}}$, where $Q_{\text{sp}} = -667$ mb and $Q_{\text{core}} = -85$ mb. The fitted value of Q_{sp} turns out to be about a factor of two larger than the expected value obtained from a neutron in the $h_{11/2}$ orbital, suggesting a strong polarization of the proton distribution.

Microscopic calculations based on a relativistic mean-field approach [14] demonstrated the relevant role played by pairing correlations that soften the stepped variations

produced by the single-particle shell structure. It was also found that the core is strongly coupled with the valence nucleons, giving rise to important core polarization contributions to the quadrupole moments.

The general trend of the isotopic evolution observed experimentally is reproduced in the present calculations. In particular, the linear increase of the quadrupole moments of the isomer $11/2^-$ states with N is obtained, although the calculations underestimate somewhat the data. In the deformed formalism, the fact that the nuclear shape of the $11/2^-$ isomers evolves from oblate to prolate with increasing neutron number has a simple explanation in terms of Nilsson-like diagrams, where one plots the single-particle energies as a function of the quadrupole deformation. The Nilsson state with asymptotic quantum numbers $[N n_z m_\ell]K = [505]11/2$ that corresponds to our $K^\pi = 11/2^-$ states, goes down (up) in energy with increasing deformation in the oblate (prolate) sector. Thus, the odd neutron in light isotopes will try to occupy that state in the oblate sector, which is lower in energy. In heavier isotopes with more neutrons occupying lower energy states, the state $[505]11/2$ will be occupied in the prolate sector.

IV. CHARGE RADII

Charge radii and their isotopic differences have been shown [31–34] to be suitable quantities to study the nuclear shape evolution as they can be measured with remarkable precision using laser spectroscopic techniques [1, 2]. One of the most noticeable characteristics of the isotopic evolution of charge radii is probably the kink that appears at shell closures. Sudden changes in the charge radii behavior are also good indicators of nuclear shape transitions taking place when the addition of a single neutron induces collective nuclear effects that drives the nucleus from a spherical into a deformed shape or vice versa. The odd-even staggering in certain neighbor isotopes is another manifestation related to the blocking effect of the odd nucleon.

There are in the literature a large variety of theoretical calculations aiming to account for the nuclear charge radii. The different approaches include phenomenological effective formulas that go beyond the simplest $r_0 A^{1/3}$ expression to various degrees of sophistication [35, 36]; Garvey-Kelson relations [37]; macroscopic-microscopic models [38–41]; and fully microscopic models either relativistic [42–44] or non-relativistic with Gogny [27, 45, 46] and Skyrme forces [23, 47].

The nuclear mean-square proton and neutron radii are defined as

$$\langle r_{p,n}^2 \rangle = \frac{\int r^2 \rho_{p,n}(\vec{r}) d\vec{r}}{\int \rho_{p,n}(\vec{r}) d\vec{r}}, \quad (3)$$

and the corresponding root-mean-square radii for protons and neutrons are simply given by

$$r_{p,n} = \langle r_{p,n}^2 \rangle^{1/2}. \quad (4)$$

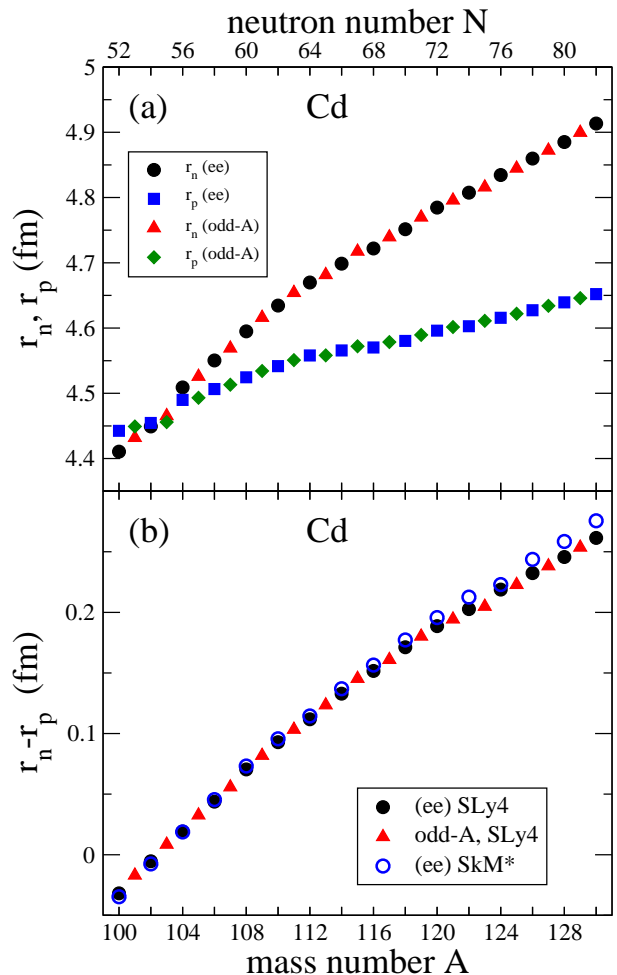


FIG. 4: (a) Neutron and proton root-mean-square radii calculated with SLy4 HF+BCS. (b) Difference $r_n - r_p$ calculated with SLy4 and SkM*.

Figure 4 shows in the upper panel (a), the neutron and proton root-mean-square radii for both even and odd Cd isotopes. Proton radii are larger than neutron radii up to $N = 54$ because of the Coulomb repulsion of the protons. For heavier isotopes the neutron radii increase more rapidly than the proton radii that still increase following the neutrons in spite of the fixed number of protons. Panel (b) shows the neutron skin thickness, $r_n - r_p$ that increases continuously as the number of neutrons increases. The figure includes also the results with SkM* that do not differ much from SLy4. Microscopic Skyrme HF+BCS calculations similar to those presented here have been performed in various isotopic chains [48–50].

The mean-square radius of the nuclear charge distribution in a nucleus is calculated by folding the proton distribution of the nucleus with the finite size of the protons and the neutrons. It can be expressed as [51, 52]

$$\langle r_c^2 \rangle = \langle r_p^2 \rangle_Z + \langle r_c^2 \rangle_p + (N/Z) \langle r_c^2 \rangle_n + r_{CM}^2 + r_{SO}^2, \quad (5)$$

where $\langle r_p^2 \rangle_Z$ is the mean-square radius of the point-proton

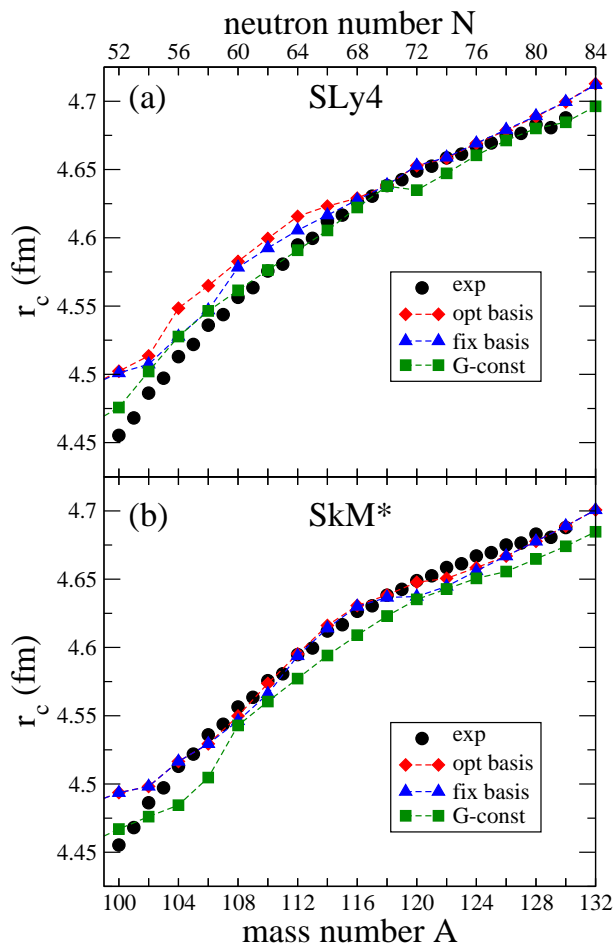


FIG. 5: Root-mean-square charge radii of the ground states in $^{100-132}\text{Cd}$ isotopes. Experimental data [13] are compared with calculations from SLy4 (a) and SkM* (b) with various theoretical treatments of the pairing and basis parameters (see text).

distribution in the nucleus given by Eq. (3). $\langle r_c^2 \rangle_p = 0.80 \text{ fm}^2$ [53] and $\langle r_c^2 \rangle_n = -0.12 \text{ fm}^2$ [54] are the mean-square radii of the charge distributions in a proton and a neutron, respectively. r_{CM}^2 is a small correction due to the center of mass motion, which is evaluated assuming harmonic-oscillator wave functions. The last term r_{SO}^2 is also a small spin-orbit contribution to the charge density. The root-mean-square charge radius of the nucleus, r_c , is simply given by

$$r_c = \langle r_c^2 \rangle^{1/2}. \quad (6)$$

It is worth noting that the most important correction to the point proton mean-square nuclear radius, coming from the charge distribution of the proton $\langle r_c^2 \rangle_p$, vanishes when isotopic differences $r^2(Z, A) - r^2(Z, A')$ are considered, since it does not involve any dependence on N . Nuclear structure effects are also canceled to a large extent in isotopic differences. In the case of radii differences between isomers and ground states $r^2(Z, A)_{\text{isomer}} - r^2(Z, A)_{\text{gs}}$, all the corrections due to fi-

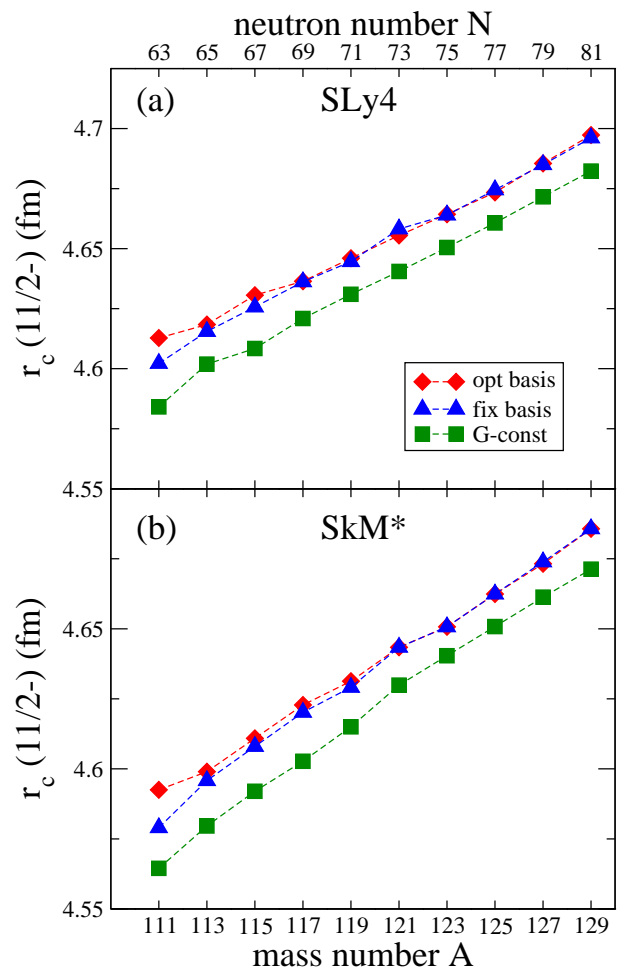


FIG. 6: Root-mean-square charge radii of the isomer $11/2^-$ states in $^{111-129}\text{Cd}$ odd- A isotopes. Calculations are from SLy4 (a) and SkM* (b) with various theoretical approaches.

nite sizes of nucleons and center of mass are canceled in the differences and only the point proton mean-square radii $\langle r_p^2 \rangle_Z$ of the isomer and ground state are involved. These radii depend only on the density of protons in the nucleus, which in turn reflects how a given number of them ($Z = 48$) are redistributed to accommodate the changing neutron environment.

Figure 5 shows the absolute values of the charge radii r_c , as measured in Ref. [13], taking $r_c(^{114}\text{Cd}) = 4.612 \text{ fm}$ as the reference radius. They are compared with the Skyrme HF+BCS results using SLy4 (a) and SkM* (b). Various theoretical treatments for the pairing interaction and different parameters of the cylindrical basis used in the expansion of the HF wave functions are considered. First, the effect of the basis is studied by comparing the results obtained with a fixed basis for all the isotopes (spherical basis with a given oscillator length) with the results obtained from an optimal choice of the deformed basis singularized for each isotope in order to minimize its energy. These results are labeled 'fix basis' and 'opt basis', respectively. Two different treatments of the pair-

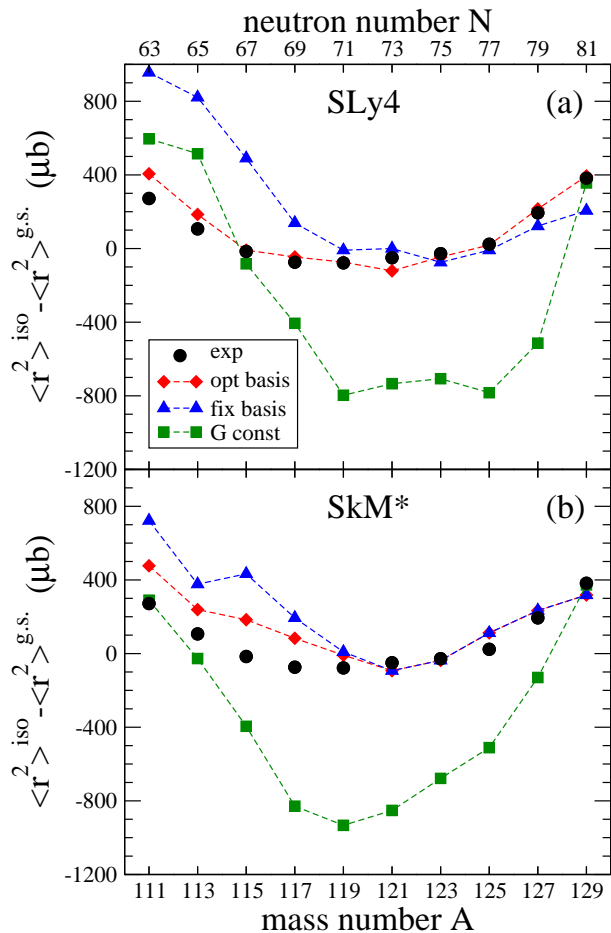


FIG. 7: Experimental mean-square charge radii differences between $11/2^-$ isomers and $1/2^+, 3/2^+$ ground states [11] compared with Skyrme HF+BCS calculations with SLy4 (a) and SkM* (b).

ing correlations are also considered by solving the BCS equations with either fixed gap parameters, fitted phenomenologically to the experimental masses, or with a fixed strength of the pairing force, labeled 'G const' in the figure.

The general trend observed experimentally is reproduced by the calculations. The results with constant G -pairing appear systematically below the results with constant pairing gaps, whereas the difference in the radii calculated with different bases is more sizable in the lighter isotopes because in this region nuclei are more deformed and therefore, the role of the deformed basis is expected to be more critical in the description of the equilibrium configurations.

Similarly, Fig. 6 shows the root-mean-square charge radii of the isomer $11/2^-$ states in the $^{111-129}\text{Cd}$ odd- A isotopes. Calculations are also from SLy4 (a) and SkM* (b) with the same theoretical approaches discussed in the previous figure for the ground-state radii. The behavior observed from different treatments of pairing and basis is similar to that in the previous figure. That is, very

similar radii with the two options for the basis, except in the lighter and deformed isotopes, and a shift to lower radii when G -pairing is considered.

As mentioned above, the variations of the charge radii patterns in isotopic chains can be related to deformation effects that can be used as signatures of shape transitions. This can be understood easily by expressing the radius as a function of deformation in a simple liquid drop model. For a nucleus with an axially symmetric static quadrupole deformation β the increase of the charge radius with respect to the radius of the spherical nucleus is given to first order by

$$\langle r^2 \rangle = \langle r^2 \rangle_{\text{sph}} \left(1 + \frac{5}{4\pi} \beta^2 \right), \quad (7)$$

where $\langle r^2 \rangle_{\text{sph}}$ is the mean-square radius of a spherical nucleus with the same volume, usually taken from the droplet model. In this work I analyze the effect of the quadrupole deformation on the charge radii from a microscopic self-consistent approach. The fact that there is a smooth evolution with no apparent jumps in Figs. 5 and 6 tells us that no sudden shape transition in the evolution of Cd isotopes is expected.

Mean-square charge radii differences between isomers and ground states in odd- A Cd isotopes were measured in Ref. [11]. A parabolic pattern of these differences was found as a function of the neutron number that was explained on the basis of a simple model as a consequence of the combination of the linear increase of the quadrupole moment of the $11/2^-$ isomer states and the rather constant behavior of the ground state quadrupole moments. The minimum of the parabola corresponds to the zero of the quadrupole moment of the isomer. It was also found that the results from a relativistic mean-field approximation support those findings [11].

The results for the charge radii differences between isomers and ground states within our HF+BCS approach are shown in Fig. 7 for SLy4 (a) and SkM* (b). The figure also explores the sensitivity of the results to the pairing force and to the parameters of the deformed basis. In general, the results with the optimal basis describe fairly well the observed parabolic behavior. The fixed basis reproduces also quite well the heavier isotopes, but becomes somewhat worse in lighter ones. As explained above, the reason for this is related to the larger deformation of lighter isotopes. The results with the constant pairing interaction show also a parabolic pattern, but they fit much worse the measurements. The pairing interaction that treats the gaps as phenomenological input parameters reproduces better the observed behavior. Results from SkM* in panel (b) are qualitatively similar.

One should keep in mind that because of the high precision achieved in the measurements of the difference between isomeric and ground state mean-square charge radii, which is of the order of $10 \mu\text{b}$ [11], the theoretical accuracy reached in present calculations of charge radii is not enough to predict unambiguously this behav-

ior. In the particular case of Cd isotopes, there is an additional difficulty because the DEC's (see Fig. 1) show rather shallow patterns around the minima. Therefore, nuclear configurations with quite different deformations have practically the same energy, but according to Eq. (7), they have different charge radii. Thus, very little changes in the input parameters of the method have almost no effect on the energies (minimizing the energy is, for example, the criterion for choosing the optimal basis), but it prevents the radii from being determined with a high level of precision.

Actually, no present theory is able to provide the level of accuracy reached experimentally. Typical mean deviations ($\bar{\epsilon} = \langle r_c(\text{theo}) - r_c(\text{exp}) \rangle$) and root-mean-square deviations ($\sigma = \langle [r_c(\text{theo}) - r_c(\text{exp})]^2 \rangle^{1/2}$) of different theoretical calculations depend of course of the sample size considered, but in general they have values around $\bar{\epsilon} = 0.001$ fm and $\sigma = 0.026$ fm in mean-field calculations with modern Skyrme interactions [47, 55]. Mean deviations of around $\bar{\epsilon} = 0.03 - 0.04$ fm are also found with the D1S and D2 Gogny interactions [46, 56]. These uncertainties are comparable to those obtained with other more phenomenological models, such as macroscopic-microscopic models [41], where values of $\sigma = 0.04 - 0.08$ fm are found; models based on Garvey-Kelson relations [37] with $\sigma = 0.01$ fm; and purely effective formulas [36], where a value $\sigma = 0.022$ fm is found. Although these theoretical uncertainties are still quite large, they are reduced to some extent when dealing with radii differences between isomers and ground states due to the cancellation of the effects of the common nuclear structure. The underlying parabolic behavior of these differences would be the signature of such cancellations. The only surviving effect would be the different quadrupole deformations of ground and isomer states, leading to the observed parabolic behavior associated with the increasing deformations from oblate to prolate in the isomers and the almost constant deformations of the ground states.

V. CONCLUSIONS

This work presents results of quadrupole moments and charge radii in even and odd $^{98-130}\text{Cd}$ isotopes. Mi-

croscopic calculations based on self-consistent deformed Skyrme Hartree-Fock with pairing are compared with high resolution laser spectroscopy experiments. In the case of odd- A isotopes, both ground states and $11/2^-$ isomeric states are studied. The main characteristics observed in the isotopic evolution, such as a linear increase of the quadrupole moments of the $11/2^-$ isomers with the number of neutrons and a parabolic behavior of the mean-square charge radii difference between isomers and ground states, are well accounted for by the calculations.

The results obtained with both Skyrme forces, SLy4 and SkM*, are qualitatively similar with a reasonable agreement with the experiment. This does not mean that other Skyrme interactions could reproduce the measurements better or that they could completely fail to do that. The results in this paper tell us that standard Skyrme forces, which are known to be quite robust to describe a large variety of nuclear properties in very different mass regions, are also suitable to explain the phenomenology observed in the charge radii behavior of Cd isotopes.

The rather shallow DEC's obtained in the isotopes of cadmium make the analysis of nuclear radii especially difficult due to the uncertainty that arises from having different deformations and, therefore, different radii with practically the same binding energy.

Although theoretical uncertainties due to different methods and approximations, or due to different interactions and parameter choices cannot compete with the high resolution achieved experimentally, still the main features observed experimentally are well described. This is specially true in the case of radii differences, where the cancellation of nuclear structure effects common to ground and isomeric states, makes evident the underlying parabolic behavior.

Acknowledgments

This work was supported by Ministerio de Ciencia, Innovación y Universidades MCIU/AEI/FEDER,UE (Spain) under Contract No. PGC2018-093636-B-I00.

-
- [1] B. Cheal and K. T. Flanagan, *J. Phys. G: Nucl. Part. Phys.* **37**, 113101 (2010).
 - [2] P. Campbell, I. D. Moore, and M. R. Pearson, *Prog. Part. Nucl. Phys.* **86**, 127 (2016).
 - [3] J. L. Wood, K. Heyde, W. Nazarewics, M. Huyse, and P. van Duppen, *Phys. Rep.* **215**, 101 (1992).
 - [4] M. Bender, P.-H. Heenen, and P.-H. Reinhard, *Rev. Mod. Phys.* **75**, 131 (2003).
 - [5] I. Angeli and K. P. Marinova, *At. Data Nucl. Data Tables* **99**, 69 (2013).
 - [6] N. J. Stone, *J. Phys. Chem. Ref. Data* **44**, 031215 (2015).
 - [7] P. E. Garrett and J. L. Wood, *J. Phys. G: Nucl. Part. Phys.* **37**, 064028 (2010); *Corrigendum* 069701.
 - [8] K. Heyde and J. L. Wood, *Rev. Mod. Phys.* **83**, 1467 (2011).
 - [9] K. Heyde, J. Jolie, R. Fossion, S. De Baerdemacker, and V. Hellemans, *Phys. Rev. C* **69**, 054304 (2004).
 - [10] D. T. Yordanov, D. L. Balabanski, J. Bieron, M. L. Bissell, K. Blaum, I. Budincevic, S. Fritzsche, N. Frömmgen, G. Georgiev, Ch. Geppert, M. Hammen, M. Kowalska, K. Kreim, A. Krieger, R. Neugart, W. Nörtershäuser, J. Papuga, and S. Schmidt, *Phys. Rev. Lett.* **110**, 192501

- (2013).
- [11] D. T. Yordanov, D. L. Balabanski, M. L. Bissell, K. Blaum, I. Budincevic, B. Cheal, K. Flanagan, N. Frömmgen, G. Georgiev, Ch. Geppert, M. Hammen, M. Kowalska, K. Kreim, A. Krieger, J. Meng, R. Neugart, G. Neyens, W. Nörtershäuser, M. M. Rajabali, J. Papuga, S. Schmidt, and P.W. Zhao, *Phys. Rev. Lett.* **116**, 032501 (2016).
- [12] D. T. Yordanov, D. L. Balabanski, M. L. Bissell, K. Blaum, A. Blazhev, I. Budincevic, N. Frömmgen, Ch. Geppert, H. Grawe, M. Hammen, K. Kreim, R. Neugart, G. Neyens, and W. Nörtershäuser, *Phys. Rev. C* **98**, 011303(R) (2018).
- [13] M. Hammen, W. Nörtershäuser, D. L. Balabanski, M. L. Bissell, K. Blaum, I. Budincevic, B. Cheal, K. T. Flanagan, N. Frömmgen, G. Georgiev, Ch. Geppert, M. Kowalska, K. Kreim, A. Krieger, W. Nazarewicz, R. Neugart, G. Neyens, J. Papuga, P.-G. Reinhard, M. M. Rajabali, S. Schmidt, and D. T. Yordanov, *Phys. Rev. Lett.* **121**, 102501 (2018).
- [14] P. W. Zhao, S. Q. Zhang, and J. Meng, *Phys. Rev. C* **89**, 011301(R) (2014).
- [15] P.-G. Reinhard and W. Nazarewicz, *Phys. Rev. C* **95**, 064328 (2017).
- [16] T. R. Rodríguez, J. L. Egidio, and A. Jungclaus, *Phys. Lett. B* **668**, 410 (2008).
- [17] K. Nomura and J. Jolie, *Phys. Rev. C* **98**, 024303 (2018).
- [18] K. Nomura, T. Otsuka, R. Rodríguez-Guzmán, L. M. Robledo, and P. Sarriguren, *Phys. Rev. C* **83**, 014309 (2011).
- [19] K. Nomura, T. Otsuka, R. Rodríguez-Guzmán, L. M. Robledo, P. Sarriguren, P. H. Regan, P. D. Stevenson, and Z. Podolyak, *Phys. Rev. C* **83**, 054303 (2011); *ibid* **84**, 054316 (2011).
- [20] E. Chabanat, P. Bonche, P. Haensel, J. Meyer, and R. Schaeffer, *Nucl. Phys. A* **635**, 231 (1998).
- [21] J. Bartel, P. Quentin, M. Brack, C. Guet, and H.-B. Hakansson, *Nucl. Phys. A* **386**, 79 (1982).
- [22] M. Dutra, O. Lourenço, J. S. Sá Martins, A. Delfino, J. R. Stone, and P. D. Stevenson, *Phys. Rev. C* **85**, 035201 (2012).
- [23] M. V. Stoitsov, J. Dobaczewski, W. Nazarewicz, S. Pittel, and D. J. Dean, *Phys. Rev. C* **68**, 054312 (2003); <https://www.fuw.edu.pl/~dobaczew/thodri/thodri.html>
- [24] D. Vautherin and D. M. Brink, *Phys. Rev. C* **5**, 626 (1972); D. Vautherin, *Phys. Rev. C* **7**, 296 (1973).
- [25] G. Audi, F. G. Kondev, M. Wang, B. Pfeiffer, X. Sun, J. Blachot, and M. MacCormick, *Chinese Phys. C* **36**, 1157 (2012); M. Wang, G. Audi, A. H. Wapstra, F. G. Kondev, M. MacCormick, X. Xu, and B. Pfeiffer, *ibid.* **36**, 1603 (2012).
- [26] H. Flocard, P. Quentin, A. K. Kerman, and D. Vautherin, *Nucl. Phys. A* **203**, 433 (1973).
- [27] S. Hilaire and M. Girod, *Eur. Phys. J. A* **33**, 237 (2007); www-phynu.cea.fr/science_en_ligne/carte_potentiels_microscopiques/carte_potentiel_nucleaire_eng.htm
- [28] R. Rodríguez-Guzmán, P. Sarriguren, and L. M. Robledo, *Phys. Rev. C* **82**, 044318 (2010).
- [29] N. Schunck, J. Dobaczewski, J. McDonnell, J. Moré, W. Nazarewicz, J. Sarich, and M. V. Stoitsov, *Phys. Rev. C* **81**, 024316 (2010).
- [30] T. Schmidt, K. L. G. Heyde, A. Blazhev, and J. Jolie, *Phys. Rev. C* **96**, 014302 (2017).
- [31] R. Rodríguez-Guzmán, P. Sarriguren, L. M. Robledo, and S. Perez-Martin, *Phys. Lett. B* **691**, 202 (2010).
- [32] R. Rodríguez-Guzmán, P. Sarriguren, and L. M. Robledo, *Phys. Rev. C* **82**, 061302(R) (2010); *Phys. Rev. C* **83**, 044307 (2011).
- [33] J. M. Boillos and P. Sarriguren, *Phys. Rev. C* **91**, 034311 (2015).
- [34] P. Sarriguren, *Phys. Rev. C* **91**, 044304 (2015).
- [35] B. Nerlo-Pomorska and K. Pomorski, *Z. Phys. A* **348**, 169 (1994).
- [36] Zongqiang Sheng, Guangwei Fan, Jianfa Qian, and Jigang Hu, *Eur. Phys. J. A* **51**, 40 (2015).
- [37] J. Piekarewicz, M. Centelles, X. Roca-Maza, and X. Viñas, *Eur. Phys. J. A* **46**, 379 (2010).
- [38] P. Möller, J. R. Nix, W. D. Myers, and W. J. Swiatecki, *At. Data Nucl. Data Tables* **59**, 185 (1995).
- [39] F. Buchinger and J. M. Pearson, *Phys. Rev. C* **72**, 057305 (2005).
- [40] H. Iimura and F. Buchinger, *Phys. Rev. C* **78**, 067301 (2008).
- [41] Hideki Iimura, Peter Möller, Takatoshi Ichikawa, Hiroyuki Sagawa, and Akira Iwamoto, *JPS Conf. Proc.* **6**, 030102 (2015).
- [42] G. A. Lalazissis, S. Raman, and P. Ring, *At. Data Nucl. Data Tables* **71**, 1 (1999).
- [43] W. Long, J. Meng, N. Van Giai, and S. G. Zhou, *Phys. Rev. C* **69**, 034319 (2004).
- [44] Lisheng Geng, Hiroshi Toki, and Jie Meng, *Prog. Theor. Phys.* **113**, 785 (2005).
- [45] J. Libert, B. Roussiere, and J. Sauvage, *Nucl. Phys. A* **786**, 47 (2007).
- [46] J.-P. Delaroche, M. Girod, J. Libert, H. Goutte, S. Hilaire, S. Péru, N. Pillet, and G. F. Bertsch, *Phys. Rev. C* **81**, 014303 (2010).
- [47] S. Goriely, N. Chamel, and J. M. Pearson, *Phys. Rev. C* **88**, 024308 (2013); <http://www-astro.ulb.ac.be/bruslib/nucdata/hfb24-dat>
- [48] P. Sarriguren, M. K. Gaidarov, E. Moya de Guerra, and A. N. Antonov, *Phys. Rev. C* **76**, 044322 (2007).
- [49] M. K. Gaidarov, A. N. Antonov, P. Sarriguren, and E. Moya de Guerra, *Phys. Rev. C* **84**, 034316 (2011); *ibid.* **85**, 064319 (2012).
- [50] M. K. Gaidarov, P. Sarriguren, A. N. Antonov, and E. Moya de Guerra, *Phys. Rev. C* **89**, 064301 (2014).
- [51] J. W. Negele, *Phys. Rev. C* **1**, 1260 (1970).
- [52] W. Bertozzi, J. Friar, J. Heisenberg, and J. W. Negele, *Phys. Lett. B* **41**, 408 (1972).
- [53] I. Sick, *Phys. Lett. B* **576**, 62 (2003).
- [54] T. R. Gentile and C. B. Crawford, *Phys. Rev. C* **83**, 055203 (2011).
- [55] S. Goriely, N. Chamel, and J. M. Pearson, *Phys. Rev. C* **93**, 034337 (2016).
- [56] N. Pillet and S. Hilaire, *Eur. Phys. J. A* **53**, 193 (2017).